RESEARCH PAPER

RNA Biology 10:3, 425–435; March 2013; © 2013 Landes Bioscience

Intermolecular domain docking in the hairpin ribozyme

Metal dependence, binding kinetics and catalysis

Minako Sumita, Neil A. White, Kristine R. Julien and Charles G. Hoogstraten*

Department of Biochemistry and Molecular Biology; Michigan State University; East Lansing, MI USA

Keywords: circular dichroism, hairpin ribozyme, RNA-cation interactions, RNA catalysis, surface plasmon resonance, ribozyme kinetics

The hairpin ribozyme is a prototype small, self-cleaving RNA motif. It exists naturally as a four-way RNA junction containing two internal loops on adjoining arms. These two loops interact in a cation-driven docking step prior to chemical catalysis to form a tightly integrated structure, with dramatic changes occurring in the conformation of each loop upon docking. We investigate the thermodynamics and kinetics of the docking process using constructs in which loop A and loop B reside on separate molecules. Using a novel CD difference assay to isolate the effects of metal ions linked to domain docking, we find the intermolecular docking process to be driven by sub-millimolar concentrations of the exchange-inert $Co(NH_3)_6^{3+}$. RNA self-cleavage requires binding of lower-affinity ions with greater apparent cooperativity than the docking process itself, implying that, even in the absence of direct coordination to RNA, metal ions play a catalytic role in hairpin ribozyme function beyond simply driving loop-loop docking. Surface plasmon resonance assays reveal remarkably slow molecular association, given the relatively tight loop-loop interaction. This observation is consistent with a "double conformational capture" model in which only collisions between loop A and loop B molecules that are simultaneously in minor, docking-competent conformations are productive for binding.

Introduction

Due to the polyanionic nature of RNA, the nature and concentrations of cations present in solution play a major role in determining the structural and functional properties of a given RNA system.[1-3] Biophysical analyses of cation binding to specific sites in RNA, however, are greatly complicated by the much larger numbers of cations interacting in non-specific or atmospheric fashion with the phosphodiester backbone.[4] Metal-dependent catalytic RNA molecules, or ribozymes, can provide an important window into cation-RNA interactions since the catalytic activity can be used as a readout for cation binding and the formation of appropriate RNA structure. The investigation of the variety of structural and functional roles played by metal ions in ribozyme mechanisms has been a fruitful source of insight into RNA structure, ribozyme function and biological catalysis in general.[5-7]

Recent years have seen substantial progress in understanding of the structures and catalytic mechanisms of ribozyme systems.[8-14] Among the best-studied catalytic RNAs are the self-cleaving ribozymes, including the hairpin and hammerhead motifs found in subviral RNAs from plant pathogenic viruses, the human hepatitis delta ribozyme, the VS ribozyme from *Neurospora crassa* and the ligand-activated *glmS* riboswitch. The hairpin ribozyme from the satellite RNA of the tobacco ringspot virus is of particular interest from a structural perspective because its active site is formed by the cation-driven interaction of two RNA internal loops to form a tightly integrated structure. In other words, an obligatory RNA tertiary structure transition, termed docking, precedes the chemical step of catalysis. In addition, full activity is observed when the physiologically relevant activating cation Mg^{2+} is replaced with the substitution-inert metal ion cobalt(III) hexamine $[Co(NH_3)_6^{3+}]$[15-17] or with very high concentrations of monovalent salts in the complete absence of polyvalent cations,[18] implying that metal ion cofactors do not play a direct role in reaction chemistry. The simplest interpretation of these results is that multivalent metal ions are required only for the formation of tertiary docked structure, but a role for metal ion cofactors in electrostatic stabilization, required conformational changes following docking or other reaction steps has not been ruled out.

The hairpin ribozyme exists naturally with loops A and B on adjoining arms of an RNA four-way junction, the presence of which greatly favors the formation of the docked state (**Fig. 1**).[19-21] The ribozyme is also highly active in a two-way junction or "minimal" form, on which much of the biochemical work has been performed.[22,23] Finally, cleavage activity has been observed with internal loops A and B on separate molecules[24,25] (**Fig. 1**). In this junctionless form, which we refer to as the "trans-docking"

*Correspondence to: Charles G. Hoogstraten; Email: hoogstr3@msu.edu
Submitted: 11/20/12; Revised: 01/11/13; Accepted: 01/14/13
http://dx.doi.org/10.4161/rna.23609

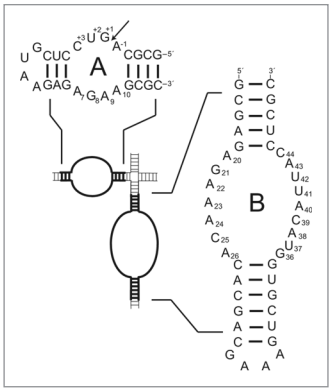

Figure 1. Hairpin ribozyme loop **A** and loop **B** constructs used in the present work shown with their context in the native, four-way junction ribozyme. Arrow indicates the site of self-cleavage.

version of the ribozyme, the docking transition represents the formation of an RNA tertiary-structure interaction in isolation from hybridization or other effects.

The hairpin ribozyme has been the subject of detailed analysis by a wide-range of biochemical and biophysical techniques,[10,11,22,26-36] notably including extensive single-molecule analysis of the docking transition.[37-40] NMR solution structures of the isolated loop A and loop B constructs have been solved,[41-43] and numerous X-ray crystallographic studies of the docked form have been performed.[11,44-52] Dramatic differences between the structures of the internal loops and of the complete ribozyme are observed, including the disruption of five of the seven noncanonical base pairs present in the solution structure of loop B,[44,53] implying extensive conformational rearrangements accompanying loop-loop interaction (**Fig. 2**). An intricate interdomain interface is formed that includes the formation of a ribose zipper, the creation of a pocket in which nucleotides from both loops envelop the base of U42 and the insertion of the loop A nucleotide G+1 (immediately 3' to the cleavage site) into the stacked structure of loop B to form a base pair with C25. The reactive groups take up the catalytically relevant in-line attack geometry in the docked structure, consistent with docking being obligatory to the formation of the active state of the ribozyme. The mechanism of domain docking is thus clearly much more complicated than a rigid lock-and-key interaction and likely involves induced fit and/or conformational-capture processes on one or both loops. Low Φ values for the formation of individual interactions measured using single-molecule techniques imply an early transition state for docking,[54] but the molecular details of the process and its driving force are not well-understood.

Biophysical studies of the hairpin ribozyme in the trans-docking form have the potential to allow new insight into the docking transition using direct measurements of bimolecular equilibrium and rate constants for binding and differential isotope labeling for spectroscopic purposes. Crystallography has confirmed that the interface in this format is essentially identical to that in the native four-way junction.[48] Although a binding constant for the loop-loop interaction under conditions of high metal ion concentration has been reported (see below), detailed biophysical characterization of this form of the ribozyme thus far is minimal.[55] In particular, there have been no reports of the metal dependence of either docking or catalysis, or of the kinetic aspects of docking, for the trans-docking reaction.

In this paper, we report equilibrium and kinetic analysis of the $Co(NH_3)_6^{3+}$-driven intermolecular docking transition in the hairpin ribozyme. To identify ionic conditions under which stable tertiary structure forms, we use a novel circular dichroism (CD) difference assay to isolate the RNA-cation interactions that are responsible for driving intermolecular docking. Using surface plasmon resonance (SPR), we observe a relatively strong (sub-micromolar K_d) binding interaction between the two domains, accompanied by remarkably slow on- and off-rates that are consistent with the dramatic structural rearrangements accompanying docking. Finally, we use assays of self-cleavage activity to compare the ionic requirements for docking and catalysis and find that, despite being unable to participate directly in reaction chemistry or Lewis acid catalysis, $Co(NH_3)_6^{3+}$ plays additional roles in the catalytic mechanism of the hairpin beyond simply driving the docking transition.

Results

Intermolecular domain docking is driven by sub-millimolar concentrations of exchange-inert trivalent metal complex. CD spectra of nucleic acids are sensitive to overall structural features, including base stacking, and have found use in studies of RNA and DNA structure and folding.[56-58] The CD spectra of loops A and B of the hairpin ribozyme would be expected to be altered upon metal ion-driven domain docking, potentially providing a useful signature for the metal dependence of docking. In a simple titration of a mixture of the two loops with $Co(NH_3)_6^{3+}$, however, this effect would be obscured by signals arising from the extensive non-specific interactions of trivalent metal ions with the polyanionic RNA backbone. Indeed, CD spectra of isolated hairpin loops showed features consistent with A-form structure that increased in intensity upon equilibration with sub-millimolar amounts of $Co(NH_3)_6^{3+}$ (**Fig. S1**). We therefore devised a novel difference CD assay to isolate the cation-binding isotherm of only those metal ion(s) whose interaction with the RNA is linked to domain docking. In this procedure (**Fig. 3**), separate CD spectra at identical $Co(NH_3)_6^{3+}$ concentrations are acquired for three samples: Loop A alone, loop B alone and a 1:1 mixture of the two molecules. Samples must be carefully dialyzed against Co-containing buffer to ensure identical concentrations of free cation (see Materials and Methods). If no interaction between the two loops occurs, the CD signal for the 1:1 mixture [$\Delta\varepsilon_{(A+B)}$] will be identical to the numerical sum of the signals for the two isolated loops ($\Delta\varepsilon_A + \Delta\varepsilon_B$) (**Fig. 3**, upper panel). To the extent that the loops interact, however, the CD spectrum of the mixture will differ from the sum of the individual loops (**Fig. 3**, lower panel). The magnitude of the difference $\Delta\Delta\varepsilon$, taken at the wavelength peak of nm, thus provides a direct readout of intermolecular domain docking. A plot of this parameter vs. [$Co(NH_3)_6^{3+}$] reveals an apparent cation-binding isotherm for only those cations whose

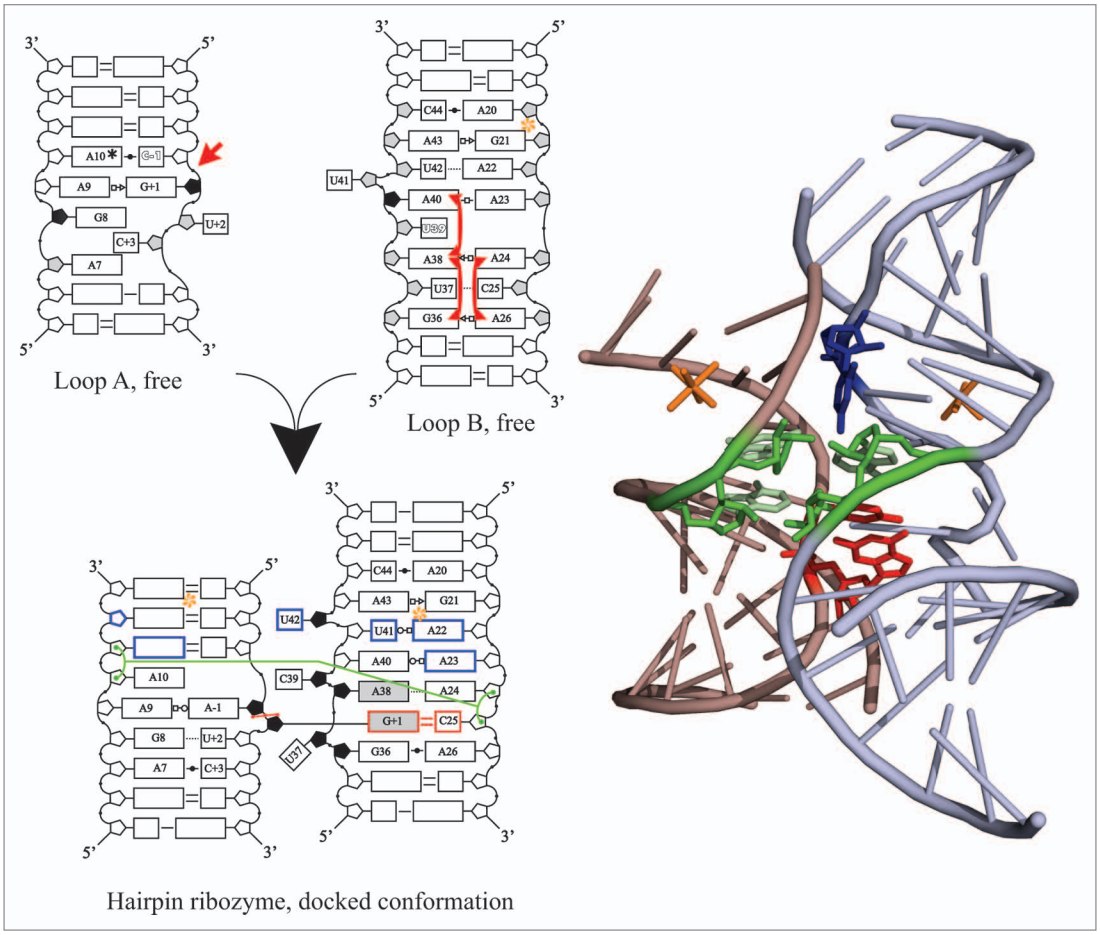

Figure 2. (**A**) Schematic of conformational changes upon formation of docked structure in the hairpin ribozyme, derived from NMR structures of the free loops[41-43] and a 2.05 Å crystal structure of the docked form in a junctionless construct.[48] Open ribose symbols are C3'-endo, shaded are C2'-endo and partly shaded (NMR structures only) display J-coupling constants characteristic of an equilibrium between the two conformations. Shading on the base moiety represents a *syn* conformation. The three major components of the interdomain interface are the G+1:C25 Watson-Crick interdomain base pair (red), a ribose zipper (green) and a complex pocket surrounding the extruded base U42 (blue). Base pair symbols are according to the convention of Leontis and Westhof,[83] in which filled symbols represent *cis* base pairs, open symbols represent *trans* (including sheared purine:purine) and circles, squares and triangles represent Watson-Crick, Hoogsteen and sugar faces, respectively. Base pairs for the crystal structure were assigned using the RNAview annotation software.[84] Asterisks (orange) indicate observed $Co(NH_3)_6^{3+}$ ions, located in the major groove in all cases. The crystallographic ion in loop B of the docked state is consistent with the location of Ca^{2+} ions in the structure of the four-way junction ribozyme[44] and with lanthanide ion cleavage data.[85] The self-cleavage site (loop **A**), NOEs inconsistent with the major conformer (loop **B**) and in-line attack conformation (docked structure) are marked. (**B**) X-ray crystallographic structure of the junctionless hairpin ribozyme (PDB 2OUE),[48] with interface elements colored to correspond with (**A**). Figure constructed with PyMOL.[86]

binding is thermodynamically linked to domain docking. The difference spectrum, unlike the CD signals of the individual samples, is unaffected by RNA-cation interactions that occur independently of domain docking.

Representative data obtained under two ionic conditions are shown in **Figure 4**. In the absence of $Co(NH_3)_6^{3+}$, domain docking was not expected to occur, and the spectrum of the mixed sample was indeed essentially identical to the sum of the spectra of the isolated loops throughout the region of the ellipticity maximum. Thus, $\Delta\Delta\varepsilon$ measurements at a particular $[Co(NH_3)_6^{3+}]$ may be presumed to arise from the effects of metal ions only. In the presence of 250 μM-free $Co(NH_3)_6^{3+}$, by contrast, a substantial shift between the two spectra was observed, leading to an easily quantifiable difference spectrum.

Measurement of $\Delta\Delta\varepsilon_{270}$ for our hairpin ribozyme constructs as a function of $[Co(NH_3)_6^{3+}]$, although perturbed by significant data scatter, resulted in an unambiguous cation-binding isotherm with a $[Co]_{½}^{dock}$ of 48.7 ± 35.0 μM (**Fig. 5**). No evidence for cooperative binding of multiple $Co(NH_3)_6^{3+}$ ions was seen, and a Hill plot of the cation-binding data (**Fig. 5**, inset) had a slope of 0.87 ± 0.63. Comparable data for the G+1A mutant of loop A showed no consistent ion-dependent changes in $\Delta\Delta\varepsilon_{270}$ (**Fig. S1**), consistent with the incompetence of this mutant for docking and strongly favoring the interpretation that the effect observed for wild-type sequences arises from authentic domain docking.

Interestingly, the $Co(NH_3)_6^{3+}$ requirements for trans-docking reported here are roughly comparable to those found by Burke and coworkers in a two-way-junction construct, which displayed

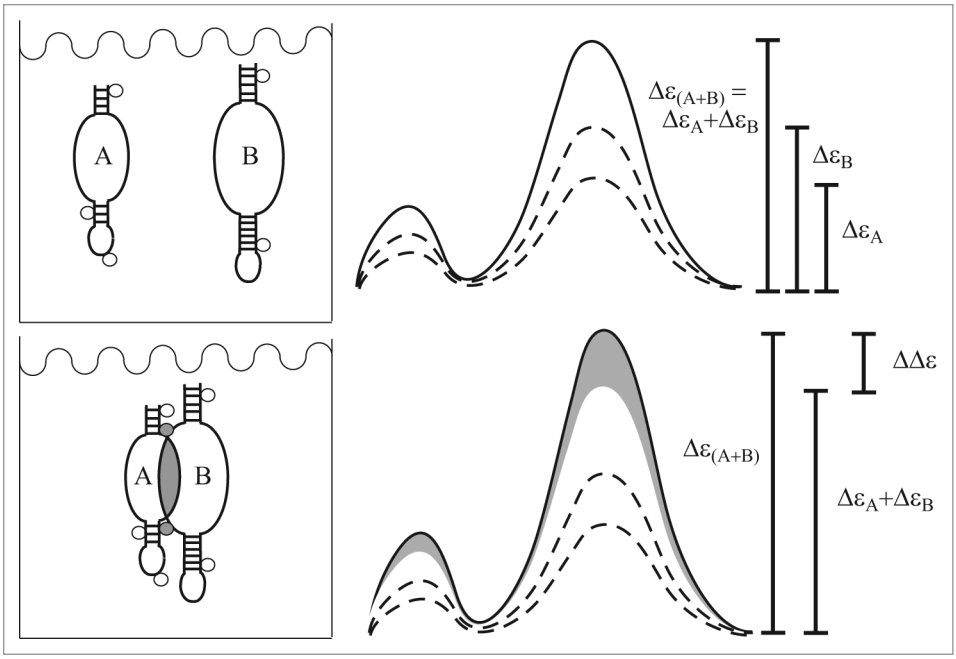

Figure 3. Schematic of the difference CD assay for the binding of ions linked to domain docking. In the absence of any docking, the observed CD spectrum of a mixture of loops **A** and **B** [$\Delta\varepsilon_{(A+B)}$, solid line] will be the arithmetic sum of those for the individual loops ($\Delta\varepsilon_A$ and $\Delta\varepsilon_B$, dashed lines) (top), whereas if docking occurs, a change in the ellipticity from that simple sum will be observed (shaded area, $\Delta\Delta\varepsilon$) (bottom). Circles indicate multivalent cations bound to RNA, shaded in the case of ions whose binding is linked to domain docking.

a $[Co]_{½}^{dock}$ of 17 ± 0.5 μM with *n* below 1.[55] By contrast, the Lilley group reported data yielding a $[Co]_{½}^{dock}$ of 0.24 μM for a four-way junction construct under somewhat different solution conditions (90 mM tris buffer pH 8.3).[59] In the latter case, a Hill coefficient of 1.75 was observed, indicating the presence of multiple cooperatively binding ions, but this effect was attributed to a known ion-binding site in the four-way junction itself, a structure not present in our experiments.[60]

Slow association and dissociation kinetics in the trans-docking hairpin ribozyme. The above results demonstrate that intermolecular domain docking is driven by relatively modest concentrations of free $Co(NH_3)_6^{3+}$. The kinetics and thermodynamics of trans-docking can thus be analyzed under saturating concentrations of trivalent metal ion. Fe-EDTA probing has previously been used to investigate the trans-docking of loops A and B under high-$[Co(NH_3)_6^{3+}]$ conditions,[55] resulting in a $K_d^{loop\ B}$ of 4.8 ± 1.8 μM. No direct measurements of docking kinetics have been reported in the junctionless form of the ribozyme, although comparisons to off-rates observed in the single-molecule context are relevant (see below).

For analysis of the kinetics of hairpin ribozyme loop-loop interactions in the trans-docking format, we used a surface plasmon resonance (SPR) assay to monitor the formation of the bound complex in real time. Chemically synthesized 5'-biotinylated wild-type loop A, rendered unreactive with a 2'-*O*-methyl modification at the nucleophilic group, was captured on one of the two SPR flow cells. Loop A with a G+1A mutation that renders the molecule inactive for both docking and catalysis was captured on the second channel as a reference. **Figure 6A** shows representative raw wild-type and mutant injection data. Both species were affected by a rapidly appearing bulk shift in refractive index, which we speculate arose from increased local concentration of high-mass cobalt complexes. A much slower, authentic macromolecular binding event was clearly present in channels containing wild-type loop A but absent in the case of the non-docking G+1A mutant. Given the dramatic difference in results upon this highly conservative sequence change, we interpret the slower event as representing the specific formation of hairpin ribozyme tertiary structure via intermolecular domain binding.

A complete SPR analysis of loop A-loop B binding at 250 μM $Co(NH_3)_6^{3+}$, at which docking reactions are driven essentially to completion (see above), is shown in **Figure 6B**. For this purpose, we plotted and fit the difference between SPR traces for wild-type loop A and G+1A mutant channels. This procedure yielded single-exponential data that could be interpreted directly in a 1:1-binding model. We observed unusually slow on- and off-rates for macromolecular interactions, with mean association rate k_a = (1.97 ± 0.29) × 10^3 M^{-1} s^{-1} and dissociation rate k_d = (7.1 ± 1.0) × 10^{-4} s^{-1}, resulting in an affinity of K_d = 372 ± 101 nM. The slow kinetics of this binding event, with an on-rate several orders of magnitude below the macromolecular diffusion limit, emphasizes the extensive conformational changes required in each domain for the formation of the docked structure (**Fig. 2**). The observed k_a is noticeably slower than previously studied RNA-RNA interactions including, for example, those for the kissing interactions between the HIV TAR RNA hairpin and either an RNA aptamer (9.2 × 10^4 M^{-1} s^{-1} at 23°C)[61] or its complementary hairpin TAR* (2.1 × 10^5 M^{-1} s^{-1} at 4°C).[62] Both of the latter processes require the unwinding of a duplex of at least five base pairs present in the unbound state for binding to occur.

Our measured K_d for the trans-docking construct is significantly more favorable than that of 4.1 ± 1.8 μM reported by Burke and coworkers using Fe-EDTA footprinting to assay the formation of the ribozyme solvent-protected core.[55] Since core protection is assumed to correlate directly with the docking interaction, this difference may arise from slight differences in ionic conditions or from minor variations in the construct, notably the use of a 2'-deoxy rather than 2'-*O*-methyl modification at the cleavage site in the footprinting work. Single-molecule kinetic fingerprinting results[63] have indicated a role for substituents at this group in modulating the loop interaction, and the precise

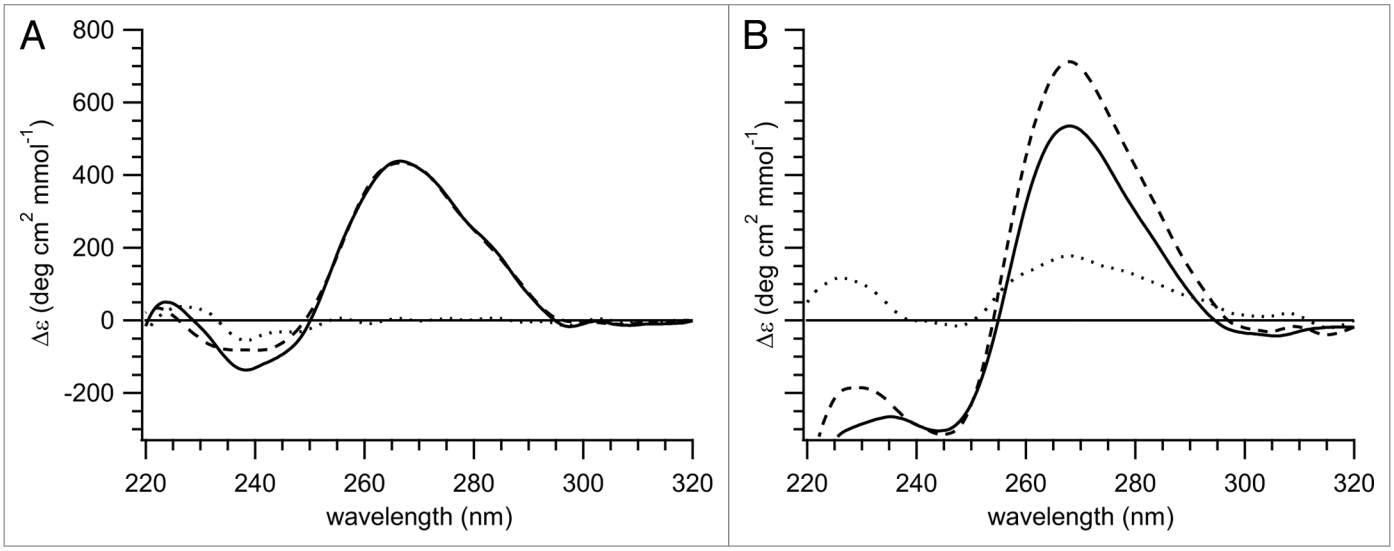

Figure 4. Comparison of CD spectra for an equimolar mixture of loops **A** and **B** [$\Delta\varepsilon_{(A+B)}$, solid line] with the arithmetic sum of spectra for the individual loops ($\Delta\varepsilon_A + \Delta\varepsilon_B$, dashed line). The difference between these traces ($\Delta\Delta\varepsilon$, dotted line) is taken as a measure of the extent of ion-driven domain docking. (**A**) Absence of $Co(NH_3)_6^{3+}$; (**B**) 250 μM free $Co(NH_3)_6^{3+}$.

effects of these modifications on on- and off-rates as well as on affinity are an interesting topic for further investigation.

Increased metal requirements for self-cleavage compared with docking. The metal activation of hairpin ribozyme self-cleavage in two- and four-way junction constructs has been extensively studied (see Introduction). In situations including the activation of a four-way junction construct with various metal ions, distinct ion dependencies for folding and cleavage have been reported.[20,59] The use of an intermolecular docking system in the present work allows a straightforward comparison of the metal dependence of domain docking, as determined above using CD, with that of ribozyme self-cleavage. These measurements take place in the absence of effects mediated by metal interactions with the junction. By considering the loop B construct as the enzyme and the loop A construct as the substrate, we determined the rate of ribozyme reaction k_{obs} under single-turnover conditions (excess of loop B over loop A) as a function of $Co(NH_3)_6^{3+}$ concentration. In all cases, essentially complete cleavage of loop A was observed at long time points (**Fig. 7**), allowing us to consider the undocking of cleaved loop A from loop B and/or the dissociation of cleavage products to be essentially irreversible. We thus neglected the effects of back-reaction in the kinetic analysis (see below). We performed most of our measurements at 500 nM loop B, which is only slightly above the K_d for the two loops determined above. However, when the 350 μM $Co(NH_3)_6^{3+}$ reaction was repeated at a loop B concentration of 3 μM, the resulting rate was identical within error to that observed at 500 nM loop B (data not shown), indicating that saturating concentrations of loop B had been reached. Consistent with this, a 10-fold lower apparent K_m vs. docking K_d was observed by Burke and co-workers,[55] possibly attributable to the difference in chemical structure at the nucleophilic oxygen (see above). At saturating concentrations of

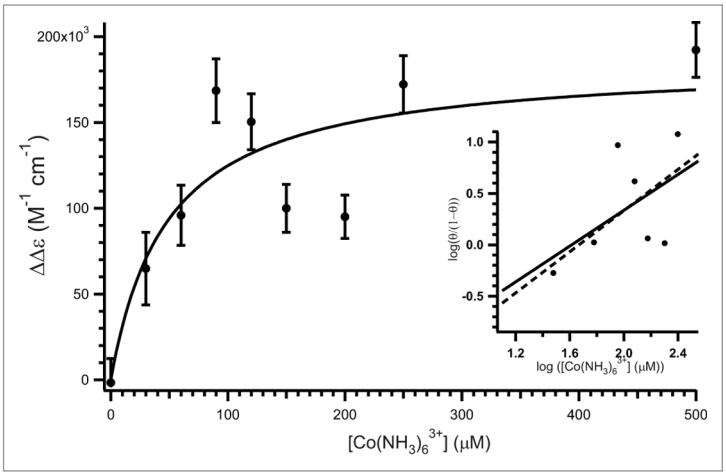

Figure 5. Binding of ions linked to domain docking as measured by difference CD analysis. Solid line, fit to equation 1. Inset, Hill plot of data through 250 μM, showing a linear fit (solid line) and a linear fit with slope forced to unity (dashed line) for comparison. Data points represent the average of results for two independently prepared samples; error bars were derived via propagation from the reproducibility of measurements on individual samples.

cation, k_{obs} reached approximately 0.1 min^{-1} (extrapolated value 0.113 ± 0.027 min^{-1}), consistent with limiting values reached in previous studies of this format.[25,55] No cleavage was observed for the control G+1A mutant of loop A (data not shown).

Our measurements showed a strongly sigmoidal dependence of k_{obs} on $[Co(NH_3)_6^{3+}]$, implying cooperative binding of multiple ions necessary for cleavage (**Fig. 8**). Fitting with **Equation 2** gave a $[Co]_{½}^{chem}$ of 168 ± 51 μM. This value is significantly higher than the $[Co]_{½}^{dock}$ observed above for interdomain docking as assayed by CD, implying that metal ions play a role in

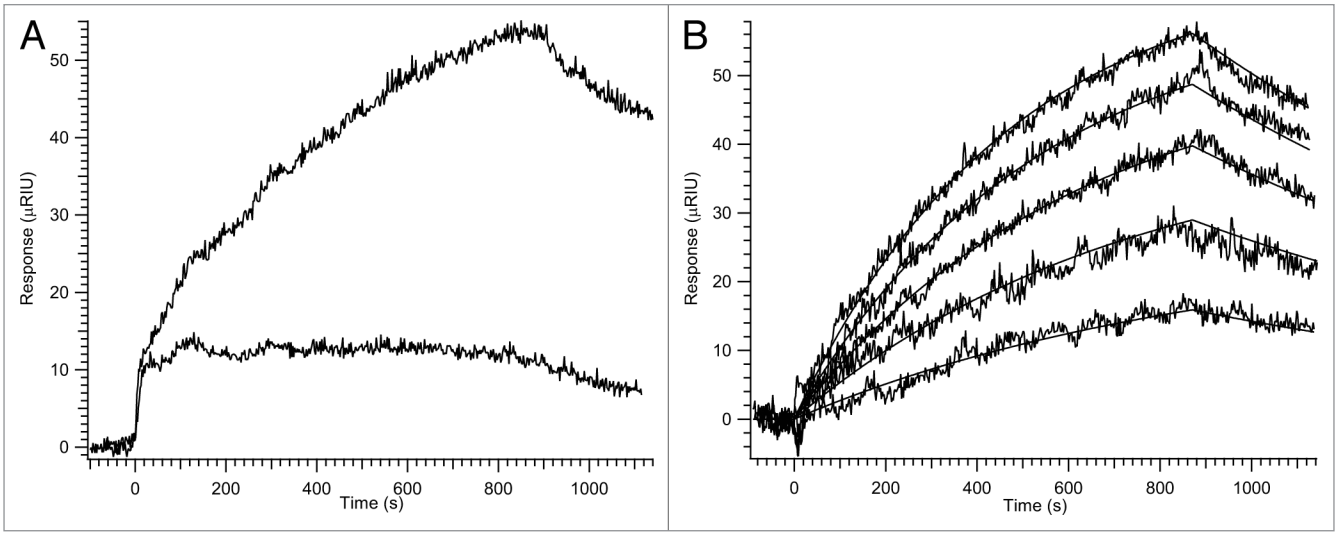

Figure 6. (**A**) Unreferenced surface plasmon resonance data acquired at 250 μM $Co(NH_3)_6^{3+}$ and 450 nM loop B. Upper trace, wild-type loop A; lower trace, G+1A mutant loop A immobilized on the same chip. (**B**) Representative fully referenced SPR analysis of domain docking at 250 μM $Co(NH_3)_6^{3+}$. Data shown are differences between a channel with immobilized wild-type loop A and one with immobilized G+1A mutant (compare left panel) and, thus, reflect only specific docking interactions. Solid lines are global fits to a 1:1 interaction model incorporating bulk refractive-index shift. Concentrations of loop B used: 150 nM, 300 nM, 450 nM, 600 nM, 750 nM.

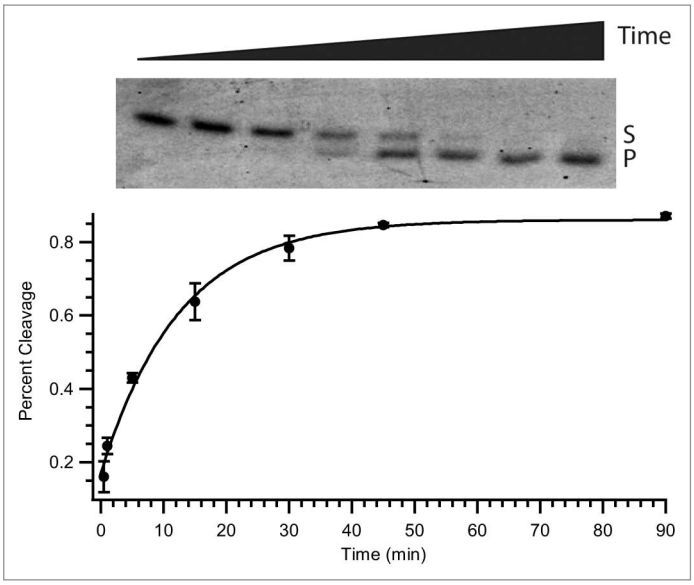

Figure 7. Cleavage kinetics of the trans-docking hairpin ribozyme at 250 μM $Co(NH_3)_6^{3+}$. Top, 20% polyacrylamide gel analysis of the cleavage of 3'-^{32}P-labeled loop A RNA, demonstrating the lack of starting material present at long time points. S, uncleaved loop A substrate (26 nucleotides); P, 3' cleavage product (21 nucleotides). Bottom, densitometric scan of the gel data fit to a single rising exponential. For this data set, the extrapolated cleavage at infinite time is 86.1%.

hairpin catalysis in this format beyond simply driving the trans-docking interaction. Consistent with this interpretation, the corresponding Hill plot exhibited linear behavior throughout the measured range with slope n of 1.87 ± 0.15, contrasting with the non-cooperative behavior observed for docking.

Interestingly, the $[Co]_{½}$ for catalysis measured here is roughly comparable to the value of 0.1 mM for a two-way junction construct (in 50 mM tris buffer pH 7.5) reported by Fedor and co-workers.[16] This result may imply that, although the ion requirements for domain docking differ greatly according to the presence and nature of the interdomain junction,[59] the binding of the final ion(s) necessary to effect catalysis proceeds with relatively little influence of the junction once the docked region has been formed. The role of the junction sequences in the hairpin ribozyme would thus contrast somewhat with that of the tertiary-stabilizing elements in the full-length hammerhead ribozyme or the kissing-loop tertiary interactions in the VS ribozyme, both of which act to dramatically decrease the ionic requirements for catalysis as well as folding.[64,65] Substantial further work would be necessary to explore this possibility fully, especially given the slightly different solution conditions between the data sets in different constructs.

Discussion

We report a detailed analysis of the thermodynamics and kinetics of intermolecular domain docking in the hairpin ribozyme activated by the exchange-inert metal complex $Co(NH_3)_6^{3+}$. We found high-affinity domain docking to be driven by sub-millimolar concentrations of free trivalent cation, with no detectable binding for a mutant previously determined to be deficient in docking, emphasizing the strong similarities between the docked states formed in native, minimal and junctionless ribozymes.[46,48] A comparison between the activation curves for stable docking and RNA self-cleavage (**Table 1**) revealed a greater ionic requirement for the latter, indicating a role in catalysis for ions binding more weakly than those directly coupled to tertiary structure formation. Similarly, the self-cleaving hammerhead ribozyme, in which metal

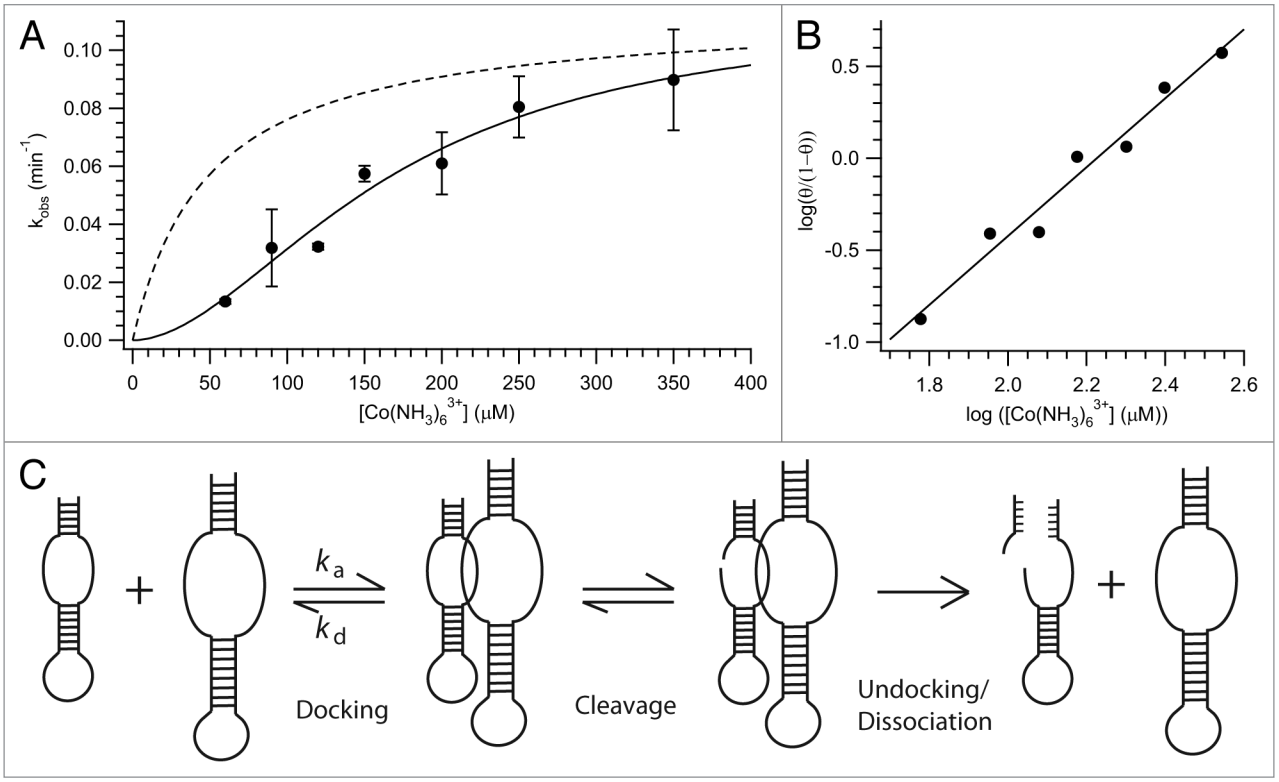

Figure 8. (A) Metal-dependent kinetics of the hairpin cleavage reaction in trans-docking format. Solid line is the fit to **Equation 2**, whereas the dashed line is the best-fit CD analysis of docking from **Figure 5** scaled to the same limiting y-value at [Co]→∞ as the kinetic data. (B) Kinetic data shown as a Hill plot. (C) Kinetic scheme for the reaction in trans-docking form indicating the observed irreversibility of undocking and/or dissociation of cleavage products (see text). Rate constants k_a and k_d correspond to those measured using SPR in this work.

ions appear to play a more direct role in catalysis than in the hairpin, has shown a distinction between ionic requirements for tertiary structure formation and self-cleavage in several contexts,[66,67] and the identity of the divalent metal used was found to strongly affect the efficiency of catalysis but not tertiary structure formation in the hammerhead.[67] In the four-way junction form of the hairpin ribozyme, multiple phases of ion-driven structure formation and distinct ionic requirements for docking and catalysis have been previously reported for Mg^{2+}-activated cleavage.[20,68] The present results refine this picture by ruling out models that explain the differential metal dependence by invoking ion interactions with junction sequences, conformational changes driven by inner-sphere ion interactions with RNA functional groups or metal ion participation in catalysis via inner-sphere effects. It is also interesting to note that Mn(II), although it does not support hairpin ribozyme self-cleavage, nevertheless leads to the formation of global tertiary structure indistinguishable from that supported by Mg^{2+} in the four-way-junction form of the ribozyme,[59] consistent with domain interaction being a necessary but not sufficient condition for cation support of catalysis in this system. The catalytic role played by ions not linked to domain docking is not known, but may involve an ion-induced conformational change of the docked structure or electrostatic participation in catalysis by ions not directly coordinated to the reactive groups.[6,59]

Although the internal equilibrium between cleavage and ligation of docked hairpin ribozymes is of order of magnitude unity under many conditions, and indeed often favors ligation,[69] we observed essentially complete cleavage of loop A at long time points in all of our kinetic assays (**Fig. 7**). We interpret this observation as arising from rapid, irreversible undocking and/or dissociation of cleavage products. Consistent with this, undocking in the two-way junction form was found via kinetic fingerprinting to be accelerated by two orders of magnitude in the cleaved (0.043 sec^{-1}) vs. the uncleaved species.[63] Likewise, undocking in the four-way-junction form is dramatically accelerated upon substrate cleavage to a rate much greater than that of religation.[70] Unless the cleavage product is much more stable to undocking in the absence than in the presence of the highly-structured junction, which we consider unlikely on structural grounds, the rate of product release in our experiments can thus be presumed to be much greater than that of religation across the full-range of $[Co(NH_3)_6^{3+}]$ values used, allowing back-reaction to be neglected. Thus, although the present results do not identify the elementary reaction step responsible for the observed ion dependence of k_{obs}, the comparisons between k_{obs} and extent of docking as measured by CD may be interpreted in straightforward fashion. The fundamental observation that at intermediate $[Co(NH_3)_6^{3+}]$ (e.g., 75 μM to 100 μM in **Fig. 8**) the extent of docking has reached a much higher fraction of its saturating value (θ = 1) than has the cleavage rate strongly supports our qualitative conclusion that cations play a role in the support of catalysis beyond that of simply driving domain docking.

Table 1. Summary comparison of metal dependence of domain docking and catalysis

	[Co]½ (μM)	n
Docking (difference CD assay)	48.7 ± 35.0	0.87 ± 0.63
Catalysis (self-cleavage assay)	167.9 ± 51.1	1.87 ± 0.15

It should be noted that phenomenological cation-binding isotherms such as those reported here do not uniquely demonstrate that individual ion(s) bind to well-defined site(s) on the nucleic acid structure. Especially under low-salt conditions, electrostatic accumulation of cations can occur in non-mass-action driven fashion, in which case $[Co]_{½}$ and n are phenomenological descriptors rather than true molecular representations of K_d and cooperativity, respectively.[2,3,71] In the isolated loop A, ion titration at concentrations leading to a substantial change in $\Delta\Delta\varepsilon$ at 270 nm (**Fig. S1**) did not significantly alter the aromatic-ribose fingerprint region of a ^{1}H-^{13}C HSQC NMR spectrum (**Fig. S2**). This observation is consistent with the lack of change in NMR data for a somewhat different loop A construct upon addition of 3 mM Mg^{2+},[41] as well as with the lack of paramagnetic broadening observed upon titration of loop A with Mn(II),[43] although both of the latter results were obtained at higher concentrations of monovalent salt than were used in this work. Regardless of the physical interpretation of the binding isotherm, however, the comparison of ionic requirements for docking and catalysis (**Fig. 8**, **Table 1**) remains valid.

Using direct on-rate measurements via SPR, we found a remarkably slow association rate between the two domains considering the relatively tight binding constant. Based on the submicromolar binding constant, we assume this association rate to correspond directly to the formation of the docked structure seen crystallographically and, thus, to probe the same process as the CD experiments. Our construct lacks the four-way junction that has been shown to be the source of the approximated but not docked state visible in some single-molecule FRET experiments.[39] A value of k_{on} five to six orders of magnitude below the diffusion limit implies, in the simplest interpretation, that only a very small fraction of encounters between loops A and B are ultimately productive for the formation of the loop-loop interaction.[72] This observation may be understood in light of the fact that both binding partners have substantial albeit dynamic structure in the undocked state (**Fig. 2**). In this situation, high-affinity binding is maintained via an extensive intermolecular interface leading to a very slow off-rate.

Although these results represent, to our knowledge, the first direct measurement of second-order rate constants for domain association in the hairpin ribozyme, it is interesting to compare the off-rate measured here with undocking rate constants (k_{undock}) previously observed in unimolecular (two-way junction) constructs. Single-molecule fluorescence resonance energy transfer (FRET) experiments have found four distinct docked states with k_{undock} varying from 0.005 sec^{-1}–3 sec^{-1} for 2'-*O*-methyl modified ribozymes in 12 mM Mg^{2+}.[37,40] Subsequent kinetic fingerprinting studies determined that k_{undock} for the most stable population decreased to 0.00045 sec^{-1} for a native, cleavable (2'-OH at A-1) substrate, emphasizing the effect of modifications at the cleavage site on the nature of the docked state.[63] The 5-fold lower off-rate measured here compared with k_{undock} for a two-way junction construct with 2'-*O*-methyl at A-1 may most likely be attributed to the greater charge on $Co(NH_3)_6^{3+}$ compared with Mg^{2+}. With this important caveat, we see no evidence for specific stabilization of the docked state by the two-way junction, consistent with the view of this structure as indistinguishable from a flexible linker.[73,74]

The measured K_d of 372 ± 101 nM corresponds to a ΔG° of -8.91 ± 0.19 kcal/mol at 30°C. This value is somewhat more negative than that typically observed in the single-molecule experiments described above, again perhaps due to different ionic conditions. Thermodynamic measurements on RNA tertiary structure formation are relatively rare, but have recently been reported for the GNRA tetraloop-tetraloop receptor complex using isothermal titration calorimetry (ITC)[75] and single-molecule[76,77] techniques. Calorimetrically determined ΔG° values in this system vary from -10.0 kcal/mol–-9.6 kcal/mol between 40°C and 47.5°C for a bivalent construct, suggesting a ΔG° of -5 kcal/mol to -6 kcal/mol for a single tetraloop-tetraloop receptor interaction at 30°C.[75] Also, for the GNRA tetraloop-tetraloop receptor complex, single-molecule techniques measured a k_{off} of more than 3 sec^{-1} at saturating Mg^{2+}, several orders of magnitude higher than that reported here for the hairpin,[78,79] emphasizing the tightly interconnected structure of the docked form of the ribozyme.

The very slow on-rate in our experiments could be explained by a model in which both isolated loops dynamically sample conformations resembling their docked states and only collisions in which each loop is simultaneously in such a state are productive for binding. Such a "double conformational capture" mechanism is not applicable in the arguably more common case in which only a single binding partner has pre-existing structure that must be disrupted for binding to occur, consistent with the relative rarity of slow binding kinetics such as observed in the hairpin. The observation of individual NOEs in isolated loop B that are consistent with the docked structure supports this possibility.[42,44] Taking advantage of the biophysical information reported here and the spectroscopic flexibility afforded by the trans-docking format, we are currently engaged in a systematic study of the dynamic properties of the isolated loops in order to explore the double conformational capture hypothesis.

Materials and Methods

RNA preparation. The following RNA sequences were used: Loop A (wild-type), 5'-GCG CAmGUCCUCGUAAGAGAGAAGCGC-3'; Loop A (G+1A), 5'- GCG CAmAUCCUCGUAAGAGAGAAGCGC-3'; Loop B, 5'-GCGAGAGAAACACACGACGAAAGUCGUGGU ACAUUACCUCGC-3'. Am indicates a 2'-*O*-methyl-adenosine modification used to preclude cleavage at the scissile phosphate. This modification was omitted in loop A sequences used for ribozyme cleavage assays. Wild-type and mutant loop A sequences (26 nt) were chemically synthesized by the W.M. Keck Foundation Biotechnology Resource laboratory at Yale University, deprotected using tetrabutylammonium fluoride (TBAF) solution

in tetrahydrofuran (THF) for 6 h at room temperature and desalted on Sephadex G-25 (Sigma-Aldrich). Loop B (42 nt) was synthesized by in vitro transcription from a synthetic DNA template with T7 RNA polymerase[80] and desalted via ethanol precipitation. Desalted RNAs were purified on a Superdex 75 (26/60) column (GE Healthcare) in which the eluent was 10 mM phosphate buffer (pH 6.5) and 100 mM NaCl at a flow rate of 3.0 mL/min.[81,82] RNA-containing fractions were combined, concentrated and desalted against RNase-free, double-deionized water using Amicon Ultra 15 centrifugal filtration units, dialyzed extensively against 20 mM HEPES, 20 μM Na_2EDTA at pH 7.5 (HPLS buffer) and finally dialyzed against HPLS containing the desired concentration of $Co(NH_3)_6^{3+}$. Dialysis was performed on a stirred Spectra/Por microdialyzer with a regenerated cellulose membrane of molecular-weight cutoff 2000. RNAs were renatured by heating to 65°C for 5 min followed by quickly cooling on ice for 10 min. For immobilization on optical chips, 5'-biotin-tagged RNAs were synthesized by Dharmacon, Inc. and deprotected according to the manufacturer's protocol. RNAs were then lyophilized and exchanged into RNase-free, double-deionized water using Amicon Ultra 4 centrifugal filtration units, analyzed for purity on a denaturing polyacrylamide gel, lyophilized to dryness and stored at -20°C. RNA was quantitated using extinction coefficients at 260 nm determined by comparison of absorbance before and after P1 nuclease digestion using the known absorbance values of the mononucleotides.[56] Final values were 214,000 M^{-1} cm^{-1} for wild-type loop A, 232,000 M^{-1} cm^{-1} for G+1A and 354,000 M^{-1} cm^{-1} for loop B. For CD samples containing 1:1 mixtures of two components, a final dialysis of at least 1 h against the desired concentration of $Co(NH_3)_6^{3+}$ was performed following mixing of the two components and the final concentration was determined using the sum of the individual extinction coefficients (i.e., changes in ε upon formation of docked structure were neglected).

Circular dichroism spectroscopy. Circular dichroism spectra were obtained with a Chirascan spectropolarimeter (Applied Photophysics). Experiments were performed in duplicate using independently dialyzed samples in HPLS buffer at 30°C and 2–3 μM RNA. Data were collected from 200–400 nm, averaged over four scans and converted to molar ellipticity (Δε) using extinction coefficients given above. Control scans of $Co(NH_3)_6^{3+}$-containing buffer samples showed negligible CD signal, justifying the neglect of contributions from free $Co(NH_3)_6^{3+}$. The binding of docking-related ions was identified according to the molar ellipticity difference (ΔΔε) at 270 nm between Δε for a sample of mixed loops A and B and the sum of Δε values for individual loop A and loop B samples. The mean deviation between duplicate determinations of ΔΔε at a single metal concentration was 12.7%. The data were fit using nonlinear regression (Igor Pro 5.04B) to where $[L]_f$ is

$$\Delta\Delta\varepsilon = \Delta\Delta\varepsilon_{max}\frac{[L]_f}{[Co]_{1/2}^{dock}+[L]_f} \quad (1)$$

the concentration of free $Co(NH_3)_6^{3+}$ as fixed by sample dialysis. Hill analysis was performed by defining θ as the ratio between ΔΔε at a given $[Co(NH_3)_6^{3+}]$ and the $\Delta\Delta\varepsilon_{max}$ extracted from the binding-isotherm curve fitting. As the measured value for ΔΔε at 500 μM [Co(III)] exceeded the extrapolated $\Delta\Delta\varepsilon_{max}$, that data point was perforce excluded from the Hill analysis. Errors are as reported by the fitting routine.

Surface plasmon resonance. Binding kinetics studies were done using a Reichert Technologies SR7000DC two-channel Surface Plasmon Resonance System at 30°C. The sensor chip used was a mixed self-assembled monolayer [10% COOH-$(EG)_6$-Alkanethiol, 90% HO-$(EG)_3$-Alkanethiol] surface (Reichert) to which streptavidin (NEB) was covalently attached using standard EDC/NHS coupling. Biotinylated wild-type and non-dockable control (G+1A) loop A were immobilized on separate channels in HPLS buffer to typical densities between 100–125 μRIU and subsequently equilibrated in HPLS with 250 μM $Co(NH_3)_6^{3+}$. Loop B samples were dialyzed for 1 h in HPLS buffer with 250 μM $Co(NH_3)_6^{3+}$ and diluted to the desired concentration in the same buffer for the kinetic experiments. SPR experiments were performed with a 15 min association phase and 10 min dissociation phase using a flow rate of 10 μL/min. Test scans indicated that results were independent of flow rate in this range. Regeneration of the baseline was achieved by injecting 1 M NaCl and ddH_2O for 10 min each. The experiment was repeated on a total of three independently prepared chip surfaces with two to three injections on each surface.

Data were analyzed using Scrubber 2 (BioLogic Software) and fit globally for each series of injections using a simple 1:1 Langmuir interaction model including bulk refractive-index shift. The signal from the reference channel [Loop A (G+1A)] was subtracted from the signal from the channel with WT Loop A to yield the specific docking. The average of multiple blank (buffer) injections was then subtracted from each curve. Rate and equilibrium constants are thus reported as mean and standard deviation of global fits to eight independent data sets.

Ribozyme kinetics. Loop A (~20 pmol) was labeled at the 3' end with (5'-^{32}P)pCp (Perkin-Elmer Life Sciences) and T4 RNA ligase (New England Biolabs Inc.) using standard methods and purified on 20% polyacrylamide gels. Cleavage reactions were performed in HPLS buffer at 30°C and were initiated by addition of $Co(NH_3)_6^{3+}$ to the desired total concentration. A typical 80 μL cleavage reaction contained ca. 5,000 cpm of labeled loop A and 500 nM loop B. For each time point, a 10 μL aliquot was removed, quenched in an equal volume of gel-loading buffer (87% formaldehyde, 25 mM Na_2EDTA, 0.02% each xylene cyanol and bromophenol blue) at 95°C for 2 min and stored on ice. The cleavage reactions were analyzed on 20% polyacrylamide gels and visualized on a Molecular Dynamics phosphorimager (GE Healthcare) with ImageQuant software (Molecular Dynamics). All experiments were repeated two or more times. The rate of hairpin ribozyme cleavage at each concentration of $Co(NH_3)_6^{3+}$ was calculated by fitting percent cleavage product present to a three-parameter rising single exponential equation (Igor Pro 5.04B). The extrapolated extent of cleavage at completion of reaction varied between 75–98%, with all but one concentration (90 μM) exceeding 85%. The resulting plot of k_{obs} vs. $[Co(NH_3)_6^{3+}]$ exhibited clear sigmoidicity (see **Fig. 8**) and was therefore fit to a cooperative binding equation:

$$k_{obs} = k_{obs,max}\frac{[L]^n}{([Co]_{1/2}^{chem})^n+[L]^n} \quad (2)$$

where [L] is the concentration of $Co(NH_3)_6^{3+}$ and n is a Hill coefficient (Igor Pro 5.04B). The reported Hill coefficient of 1.87 ± 0.15 was extracted from the slope of a linear Hill plot of the data and was identical within error to that obtained from direct fitting to **Equation 2** (1.86 ± 0.55). Errors in $[Co]_{1/2}^{chem}$ and n are as reported by the fitting routines.

Disclosure of Potential Conflicts of Interest

No potential conflicts of interest were disclosed.

Acknowledgments

This work was supported by the U.S. National Institutes of Health (GM069742 to C.G.H.). The authors are grateful to Nils Walter and Philip Bevilacqua for many helpful discussions, Lisa Lapidus for the use of the Chirascan CD instrument and Vijay Singh for assistance with its operation, Philip Page of Reichert Instruments for assistance with SPR technology and John Wang and Patricia Voss for support of ^{32}P experimentation.

Supplemental Materials

Supplemental material may be found here:
www.landesbioscience.com/journals/rnabiology/article/23609

References

1. Leroy JL, Guéron M. Electrostatic effects in divalent ion binding to tRNA. Biopolymers 1977; 16:2429-46; PMID:334280; http://dx.doi.org/10.1002/bip.1977.360161108.
2. Draper DE. A guide to ions and RNA structure. RNA 2004; 10:335-43; PMID:14970378; http://dx.doi.org/10.1261/rna.5205404.
3. Draper DE, Grilley D, Soto AM. Ions and RNA folding. Annu Rev Biophys Biomol Struct 2005; 34:221-43; PMID:15869389; http://dx.doi.org/10.1146/annurev.biophys.34.040204.144511.
4. Narlikar GJ, Herschlag D. Mechanistic aspects of enzymatic catalysis: lessons from comparison of RNA and protein enzymes. Annu Rev Biochem 1997; 66:19-59; PMID:9242901; http://dx.doi.org/10.1146/annurev.biochem.66.1.19.
5. Pyle AM. Metal ions in the structure and function of RNA. J Biol Inorg Chem 2002; 7:679-90; PMID:12203005; http://dx.doi.org/10.1007/s00775-002-0387-6.
6. Sigel RK, Pyle AM. Alternative roles for metal ions in enzyme catalysis and the implications for ribozyme chemistry. Chem Rev 2007; 107:97-113; PMID:17212472; http://dx.doi.org/10.1021/cr0502605.
7. Johnson-Buck AE, McDowell SE, Walter NG. Metal ions: supporting actors in the playbook of small ribozymes. Met Ions Life Sci 2011; 9:175-96; PMID:22010272; http://dx.doi.org/10.1039/9781849732512-00175.
8. Hoogstraten CG, Sumita M. Structure-function relationships in RNA and RNP enzymes: recent advances. Biopolymers 2007; 87:317-28; PMID:17806104; http://dx.doi.org/10.1002/bip.20836.
9. Hougland JL, Piccirilli JA, Forconi M, Lee J, Herschlag D. How the group I intron works: A case study of RNA structure and function, In: Gesteland RF, Cech TR, Atkins JF, eds. The RNA World. Cold Spring Harbor, NY, USA: Cold Spring Harbor Laboratory Press, 2006: 133-206.
10. Cochrane JC, Strobel SA. Catalytic strategies of self-cleaving ribozymes. Acc Chem Res 2008; 41:1027-35; PMID:18652494; http://dx.doi.org/10.1021/ar800050c.
11. Fedor MJ. Comparative enzymology and structural biology of RNA self-cleavage. Annu Rev Biophys 2009; 38:271-99; PMID:19416070; http://dx.doi.org/10.1146/annurev.biophys.050708.133710.
12. Lilley DM. Mechanisms of RNA catalysis. Philos Trans R Soc Lond B Biol Sci 2011; 366:2910-7; PMID:21930582; http://dx.doi.org/10.1098/rstb.2011.0132.
13. Lilley DM. Catalysis by the nucleolytic ribozymes. Biochem Soc Trans 2011; 39:641-6; PMID:21428954; http://dx.doi.org/10.1042/BST0390641.
14. Reymond C, Beaudoin JD, Perreault JP. Modulating RNA structure and catalysis: lessons from small cleaving ribozymes. Cell Mol Life Sci 2009; 66:3937-50; PMID:19718544; http://dx.doi.org/10.1007/s00018-009-0124-1.
15. Hampel A, Cowan JA. A unique mechanism for RNA catalysis: the role of metal cofactors in hairpin ribozyme cleavage. Chem Biol 1997; 4:513-7; PMID:9263639; http://dx.doi.org/10.1016/S1074-5521(97)90323-9.
16. Nesbitt S, Hegg LA, Fedor MJ. An unusual pH-independent and metal-ion-independent mechanism for hairpin ribozyme catalysis. Chem Biol 1997; 4:619-30; PMID:9281529; http://dx.doi.org/10.1016/S1074-5521(97)90247-7.
17. Young KJ, Gill F, Grasby JA. Metal ions play a passive role in the hairpin ribozyme catalysed reaction. Nucleic Acids Res 1997; 25:3760-6; PMID:9380495; http://dx.doi.org/10.1093/nar/25.19.3760.
18. Murray JB, Seyhan AA, Walter NG, Burke JM, Scott WG. The hammerhead, hairpin and VS ribozymes are catalytically proficient in monovalent cations alone. Chem Biol 1998; 5:587-95; PMID:9818150; http://dx.doi.org/10.1016/S1074-5521(98)90116-8.
19. Murchie AI, Thomson JB, Walter F, Lilley DM. Folding of the hairpin ribozyme in its natural conformation achieves close physical proximity of the loops. Mol Cell 1998; 1:873-81; PMID:9660970; http://dx.doi.org/10.1016/S1097-2765(00)80086-6.
20. Thomson JB, Lilley DM. The influence of junction conformation on RNA cleavage by the hairpin ribozyme in its natural junction form. RNA 1999; 5:180-7; PMID:10024170; http://dx.doi.org/10.1017/S1355838299981670.
21. Walter NG, Burke JM, Millar DP. Stability of hairpin ribozyme tertiary structure is governed by the interdomain junction. Nat Struct Biol 1999; 6:544-9; PMID:10360357; http://dx.doi.org/10.1038/9316.
22. Walter NG, Burke JM. The hairpin ribozyme: structure, assembly and catalysis. Curr Opin Chem Biol 1998; 2:24-30; PMID:9667918; http://dx.doi.org/10.1016/S1367-5931(98)80032-X.
23. Fedor MJ. The catalytic mechanism of the hairpin ribozyme. Biochem Soc Trans 2002; 30:1109-15; PMID:12440984; http://dx.doi.org/10.1042/BST0301109.
24. Butcher SE, Heckman JE, Burke JM. Reconstitution of hairpin ribozyme activity following separation of functional domains. J Biol Chem 1995; 270:29648-51; PMID:8530348; http://dx.doi.org/10.1074/jbc.270.50.29648.
25. Shin C, Choi JN, Song SI, Song JT, Ahn JH, Lee JS, et al. The loop B domain is physically separable from the loop A domain in the hairpin ribozyme. Nucleic Acids Res 1996; 24:2685-9; PMID:8758996; http://dx.doi.org/10.1093/nar/24.14.2685.
26. Fedor MJ. The catalytic mechanism of the hairpin ribozyme. Biochem Soc Trans 2002; 30:1109-15; PMID:12440984; http://dx.doi.org/10.1042/BST0301109.
27. Fedor MJ, Williamson JR. The catalytic diversity of RNAs. Nat Rev Mol Cell Biol 2005; 6:399-412; PMID:15956979; http://dx.doi.org/10.1038/nrm1647.
28. Ferré-D'Amaré AR. The hairpin ribozyme. Biopolymers 2004; 73:71-8; PMID:14691941; http://dx.doi.org/10.1002/bip.10516.
29. Wilson TJ, Nahas M, Ha T, Lilley DM. Folding and catalysis of the hairpin ribozyme. Biochem Soc Trans 2005; 33:461-5; PMID:15916541; http://dx.doi.org/10.1042/BST0330461.
30. Nam K, Gao J, York DM. Quantum mechanical/molecular mechanical simulation study of the mechanism of hairpin ribozyme catalysis. J Am Chem Soc 2008; 130:4680-91; PMID:18345664; http://dx.doi.org/10.1021/ja0759141.
31. Guo M, Spitale RC, Volpini R, Krucinska J, Cristalli G, Carey PR, et al. Direct Raman measurement of an elevated base pKa in the active site of a small ribozyme in a precatalytic conformation. J Am Chem Soc 2009; 131:12908-9; PMID:19702306; http://dx.doi.org/10.1021/ja9060883.
32. Suydam IT, Levandoski SD, Strobel SA. Catalytic importance of a protonated adenosine in the hairpin ribozyme active site. Biochemistry 2010; 49:3723-32; PMID:20373826; http://dx.doi.org/10.1021/bi100234v.
33. Wilson TJ, Lilley DM. Do the hairpin and VS ribozymes share a common catalytic mechanism based on general acid-base catalysis? A critical assessment of available experimental data. RNA 2011; 17:213-21; PMID:21173201; http://dx.doi.org/10.1261/rna.2473711.
34. Kath-Schorr S, Wilson TJ, Li NS, Lu J, Piccirilli JA, Lilley DM. General acid-base catalysis mediated by nucleobases in the hairpin ribozyme. J Am Chem Soc 2012; 134:16717-24; PMID:22958171; http://dx.doi.org/10.1021/ja3067429.
35. Mlýnský V, Banás P, Hollas D, Réblová K, Walter NG, Sponer J, et al. Extensive molecular dynamics simulations showing that canonical G8 and protonated A38H+ forms are most consistent with crystal structures of hairpin ribozyme. J Phys Chem B 2010; 114:6642-52; PMID:20420375; http://dx.doi.org/10.1021/jp1001258.
36. Mlýnský V, Banáš P, Walter NG, Šponer J, Otyepka M. QM/MM studies of hairpin ribozyme self-cleavage suggest the feasibility of multiple competing reaction mechanisms. J Phys Chem B 2011; 115:13911-24; PMID:22014231; http://dx.doi.org/10.1021/jp206963g.
37. Zhuang X, Kim H, Pereira MJ, Babcock HP, Walter NG, Chu S. Correlating structural dynamics and function in single ribozyme molecules. Science 2002; 296:1473-6; PMID:12029135; http://dx.doi.org/10.1126/science.1069013.
38. Ditzler MA, Alemán EA, Rueda D, Walter NG. Focus on function: single molecule RNA enzymology. Biopolymers 2007; 87:302-16; PMID:17685395; http://dx.doi.org/10.1002/bip.20819.

39. Wilson TJ, Nahas M, Araki L, Harusawa S, Ha T, Lilley DM. RNA folding and the origins of catalytic activity in the hairpin ribozyme. Blood Cells Mol Dis 2007; 38:8-14; PMID:17150385; http://dx.doi.org/10.1016/j.bcmd.2006.10.004.
40. Ditzler MA, Rueda D, Mo J, Håkansson K, Walter NG. A rugged free energy landscape separates multiple functional RNA folds throughout denaturation. Nucleic Acids Res 2008; 36:7088-99; PMID:18988629; http://dx.doi.org/10.1093/nar/gkn871.
41. Cai Z, Tinoco I Jr. Solution structure of loop A from the hairpin ribozyme from tobacco ringspot virus satellite. Biochemistry 1996; 35:6026-36; PMID:8634244; http://dx.doi.org/10.1021/bi952985g.
42. Butcher SE, Allain FH, Feigon J. Solution structure of the loop B domain from the hairpin ribozyme. Nat Struct Biol 1999; 6:212-6; PMID:10074938; http://dx.doi.org/10.1038/6651.
43. Butcher SE, Allain FH, Feigon J. Determination of metal ion binding sites within the hairpin ribozyme domains by NMR. Biochemistry 2000; 39:2174-82; PMID:10694382; http://dx.doi.org/10.1021/bi9923454.
44. Rupert PB, Ferré-D'Amaré AR. Crystal structure of a hairpin ribozyme-inhibitor complex with implications for catalysis. Nature 2001; 410:780-6; PMID:11298439; http://dx.doi.org/10.1038/35071009.
45. Rupert PB, Massey AP, Sigurdsson ST, Ferré-D'Amaré AR. Transition state stabilization by a catalytic RNA. Science 2002; 298:1421-4; PMID:12376595; http://dx.doi.org/10.1126/science.1076093.
46. Grum-Tokars V, Milovanovic M, Wedekind JE. Crystallization and X-ray diffraction analysis of an all-RNA $U_{39}C$ mutant of the minimal hairpin ribozyme. Acta Crystallogr D Biol Crystallogr 2003; 59:142-5; PMID:12499551; http://dx.doi.org/10.1107/S0907444902019066.
47. Alam S, Grum-Tokars V, Krucinska J, Kundracik ML, Wedekind JE. Conformational heterogeneity at position U37 of an all-RNA hairpin ribozyme with implications for metal binding and the catalytic structure of the S-turn. Biochemistry 2005; 44:14396-408; PMID:16262240; http://dx.doi.org/10.1021/bi051550i.
48. Salter J, Krucinska J, Alam S, Grum-Tokars V, Wedekind JE. Water in the active site of an all-RNA hairpin ribozyme and effects of Gua8 base variants on the geometry of phosphoryl transfer. Biochemistry 2006; 45:686-700; PMID:16411744; http://dx.doi.org/10.1021/bi051887k.
49. Torelli AT, Krucinska J, Wedekind JE. A comparison of vanadate to a 2'-5' linkage at the active site of a small ribozyme suggests a role for water in transition-state stabilization. RNA 2007; 13:1052-70; PMID:17488874; http://dx.doi.org/10.1261/rna.510807.
50. Spitale RC, Wedekind JE. Exploring ribozyme conformational changes with X-ray crystallography. Methods 2009; 49:87-100; PMID:19559088; http://dx.doi.org/10.1016/j.ymeth.2009.06.003.
51. Spitale RC, Volpini R, Heller MG, Krucinska J, Cristalli G, Wedekind JE. Identification of an imino group indispensable for cleavage by a small ribozyme. J Am Chem Soc 2009; 131:6093-5; PMID:19354216; http://dx.doi.org/10.1021/ja900450h.
52. Liberman JA, Guo M, Jenkins JL, Krucinska J, Chen Y, Carey PR, et al. A transition-state interaction shifts nucleobase ionization toward neutrality to facilitate small ribozyme catalysis. J Am Chem Soc 2012; 134:16933-6; PMID:22989273; http://dx.doi.org/10.1021/ja3070528.
53. Ferré-D'amaré AR, Rupert PB. The hairpin ribozyme: from crystal structure to function. Biochem Soc Trans 2002; 30:1105-9; PMID:12440983; http://dx.doi.org/10.1042/BST0301105.
54. Bokinsky G, Rueda D, Misra VK, Rhodes MM, Gordus A, Babcock HP, et al. Single-molecule transition-state analysis of RNA folding. Proc Natl Acad Sci USA 2003; 100:9302-7; PMID:12869691; http://dx.doi.org/10.1073/pnas.1133280100.
55. Hampel KJ, Walter NG, Burke JM. The solvent-protected core of the hairpin ribozyme-substrate complex. Biochemistry 1998; 37:14672-82; PMID:9778342; http://dx.doi.org/10.1021/bi981083n.
56. Gray DM, Hung SH, Johnson KH. Absorption and circular dichroism spectroscopy of nucleic acid duplexes and triplexes. Methods Enzymol 1995; 246:19-34; PMID:7538624; http://dx.doi.org/10.1016/0076-6879(95)46005-5.
57. Sosnick TR, Fang X, Shelton VM. Application of circular dichroism to study RNA folding transitions. Methods Enzymol 2000; 317:393-409; PMID:10829292; http://dx.doi.org/10.1016/S0076-6879(00)17026-0.
58. Kypr J, Kejnovská I, Renciuk D, Vorlícková M. Circular dichroism and conformational polymorphism of DNA. Nucleic Acids Res 2009; 37:1713-25; PMID:19190094; http://dx.doi.org/10.1093/nar/gkp026.
59. Walter F, Murchie AI, Thomson JB, Lilley DM. Structure and activity of the hairpin ribozyme in its natural junction conformation: effect of metal ions. Biochemistry 1998; 37:14195-203; PMID:9760257; http://dx.doi.org/10.1021/bi981513+.
60. Walter F, Murchie AI, Lilley DM. Folding of the four-way RNA junction of the hairpin ribozyme. Biochemistry 1998; 37:17629-36; PMID:9860879; http://dx.doi.org/10.1021/bi9821115.
61. Lebars I, Legrand P, Aimé A, Pinaud N, Fribourg S, Di Primo C. Exploring TAR-RNA aptamer loop-loop interaction by X-ray crystallography, UV spectroscopy and surface plasmon resonance. Nucleic Acids Res 2008; 36:7146-56; PMID:18996893; http://dx.doi.org/10.1093/nar/gkn831.
62. Nair TM, Myszka DG, Davis DR. Surface plasmon resonance kinetic studies of the HIV TAR RNA kissing hairpin complex and its stabilization by 2-thiouridine modification. Nucleic Acids Res 2000; 28:1935-40; PMID:10756194; http://dx.doi.org/10.1093/nar/28.9.1935.
63. Liu S, Bokinsky G, Walter NG, Zhuang X. Dissecting the multistep reaction pathway of an RNA enzyme by single-molecule kinetic "fingerprinting". Proc Natl Acad Sci USA 2007; 104:12634-9; PMID:17496145; http://dx.doi.org/10.1073/pnas.0610597104.
64. Penedo JC, Wilson TJ, Jayasena SD, Khvorova A, Lilley DM. Folding of the natural hammerhead ribozyme is enhanced by interaction of auxiliary elements. RNA 2004; 10:880-8; PMID:15100442; http://dx.doi.org/10.1261/rna.5268404.
65. DeAbreu DM, Olive JE, Collins RA. Additional roles of a peripheral loop-loop interaction in the Neurospora VS ribozyme. Nucleic Acids Res 2011; 39:6223-8; PMID:21507887; http://dx.doi.org/10.1093/nar/gkr250.
66. Kim NK, Murali A, DeRose VJ. Separate metal requirements for loop interactions and catalysis in the extended hammerhead ribozyme. J Am Chem Soc 2005; 127:14134-5; PMID:16218578; http://dx.doi.org/10.1021/ja0541027.
67. Boots JL, Canny MD, Azimi E, Pardi A. Metal ion specificities for folding and cleavage activity in the Schistosoma hammerhead ribozyme. RNA 2008; 14:2212-22; PMID:18755844; http://dx.doi.org/10.1261/rna.1010808.
68. Wilson TJ, Lilley DM. Metal ion binding and the folding of the hairpin ribozyme. RNA 2002; 8:587-600; PMID:12022226; http://dx.doi.org/10.1017/S1355838202020514.
69. Nesbitt SM, Erlacher HA, Fedor MJ. The internal equilibrium of the hairpin ribozyme: temperature, ion and pH effects. J Mol Biol 1999; 286:1009-24; PMID:10047478; http://dx.doi.org/10.1006/jmbi.1999.2543.
70. Nahas MK, Wilson TJ, Hohng S, Jarvie K, Lilley DM, Ha T. Observation of internal cleavage and ligation reactions of a ribozyme. Nat Struct Mol Biol 2004; 11:1107-13; PMID:15475966; http://dx.doi.org/10.1038/nsmb842.
71. Leipply D, Draper DE. Dependence of RNA tertiary structural stability on Mg2+ concentration: interpretation of the Hill equation and coefficient. Biochemistry 2010; 49:1843-53; PMID:20112919; http://dx.doi.org/10.1021/bi902036j.
72. Berg OG, von Hippel PH. Diffusion-controlled macromolecular interactions. Annu Rev Biophys Biophys Chem 1985; 14:131-60; PMID:3890878; http://dx.doi.org/10.1146/annurev.bb.14.060185.001023.
73. Rueda D, Bokinsky G, Rhodes MM, Rust MJ, Zhuang X, Walter NG. Single-molecule enzymology of RNA: essential functional groups impact catalysis from a distance. Proc Natl Acad Sci USA 2004; 101:10066-71; PMID:15218105; http://dx.doi.org/10.1073/pnas.0403575101.
74. MacElrevey C, Spitale RC, Krucinska J, Wedekind JE. A posteriori design of crystal contacts to improve the X-ray diffraction properties of a small RNA enzyme. Acta Crystallogr D Biol Crystallogr 2007; 63:812-25; PMID:17582172; http://dx.doi.org/10.1107/S090744490702464X.
75. Vander Meulen KA, Davis JH, Foster TR, Record MT Jr., Butcher SE. Thermodynamics and folding pathway of tetraloop receptor-mediated RNA helical packing. J Mol Biol 2008; 384:702-17; PMID:18845162; http://dx.doi.org/10.1016/j.jmb.2008.09.049.
76. Fiore JL, Hodak JH, Piestert O, Downey CD, Nesbitt DJ. Monovalent and divalent promoted GAAA tetraloop-receptor tertiary interactions from freely diffusing single-molecule studies. Biophys J 2008; 95:3892-905; PMID:18621836; http://dx.doi.org/10.1529/biophysj.108.134346.
77. Fiore JL, Kraemer B, Koberling F, Edmann R, Nesbitt DJ. Enthalpy-driven RNA folding: single-molecule thermodynamics of tetraloop-receptor tertiary interaction. Biochemistry 2009; 48:2550-8; PMID:19186984; http://dx.doi.org/10.1021/bi8019788.
78. Hodak JH, Downey CD, Fiore JL, Pardi A, Nesbitt DJ. Docking kinetics and equilibrium of a GAAA tetraloop-receptor motif probed by single-molecule FRET. Proc Natl Acad Sci USA 2005; 102:10505-10; PMID:16024731; http://dx.doi.org/10.1073/pnas.0408645102.
79. Downey CD, Fiore JL, Stoddard CD, Hodak JH, Nesbitt DJ, Pardi A. Metal ion dependence, thermodynamics, and kinetics for intramolecular docking of a GAAA tetraloop and receptor connected by a flexible linker. Biochemistry 2006; 45:3664-73; PMID:16533049; http://dx.doi.org/10.1021/bi0520941.
80. Milligan JF, Groebe DR, Witherell GW, Uhlenbeck OC. Oligoribonucleotide synthesis using T7 RNA polymerase and synthetic DNA templates. Nucleic Acids Res 1987; 15:8783-98; PMID:3684574; http://dx.doi.org/10.1093/nar/15.21.8783.
81. Kim I, McKenna SA, Viani Puglisi E, Puglisi JD. Rapid purification of RNAs using fast performance liquid chromatography (FPLC). RNA 2007; 13:289-94; PMID:17179067; http://dx.doi.org/10.1261/rna.342607.
82. McKenna SA, Kim I, Puglisi EV, Lindhout DA, Aitken CE, Marshall RA, et al. Purification and characterization of transcribed RNAs using gel filtration chromatography. Nat Protoc 2007; 2:3270-7; PMID:18079727; http://dx.doi.org/10.1038/nprot.2007.480.
83. Leontis NB, Westhof E. Geometric nomenclature and classification of RNA base pairs. RNA 2001; 7:499-512; PMID:11345429; http://dx.doi.org/10.1017/S1355838201002515.
84. Yang H, Jossinet F, Leontis N, Chen L, Westbrook J, Berman H, et al. Tools for the automatic identification and classification of RNA base pairs. Nucleic Acids Res 2003; 31:3450-60; PMID:12824344; http://dx.doi.org/10.1093/nar/gkg529.
85. Walter NG, Yang N, Burke JM. Probing non-selective cation binding in the hairpin ribozyme with Tb(III). J Mol Biol 2000; 298:539-55; PMID:10772868; http://dx.doi.org/10.1006/jmbi.2000.3691.
86. Delano WL. The PyMOL Molecular Graphics System. Palo Alto, CA, USA: DeLano Scientific, 2002.